



Full length article

A satellite-driven model to estimate long-term particulate sulfate levels and attributable mortality burden in China



Xia Meng^{a,1}, Yun Hang^{b,1}, Xiuran Lin^b, Tiantian Li^c, Tijian Wang^d, Junji Cao^e, Qingyan Fu^f, Sagnik Dey^g, Kan Huang^h, Fengchao Liangⁱ, Haidong Kan^a, Xiaoming Shi^{c,*}, Yang Liu^{b,*}

^a School of Public Health, Fudan University, Shanghai 200032, China

^b Gangarosa Department of Environmental Health, Rollins School of Public Health, Emory University, Atlanta, GA 30322, USA

^c China CDC Key Laboratory of Environment and Population Health, National Institute of Environmental Health, Chinese Center for Disease Control and Prevention, Beijing, 100021, China

^d School of Atmospheric Sciences, Nanjing University, Nanjing 210023, China

^e Key Laboratory of Aerosol Chemistry and Physics, State Key Laboratory of Loess and Quaternary Geology, Institute of Earth Environment, Chinese Academy of Sciences, CAS Center for Excellence in Quaternary Science and Global Change, Shaanxi Key Laboratory of Atmospheric and Haze-fog Pollution Prevention, Xi'an 710061, China

^f State Ecologic Environmental Scientific Observation and Research Station at Dianshan Lake, Shanghai Environmental Monitoring Center, Shanghai 200235, China

^g Centre for Atmospheric Sciences, Indian Institute of Technology Delhi, Hauz Khas, New Delhi 110016, India

^h Shanghai Key Laboratory of Atmospheric Particle Pollution and Prevention (LAP3), Department of Environmental Science and Engineering, Fudan University, Shanghai 200433, China

ⁱ School of Public Health and Emergency Management, Southern University of Science and Technology, Shenzhen 518055, China

ARTICLE INFO

Handling Editor: Adrian Covaci

Keywords:

Air pollution
Particulate sulfate
Atmospheric big data
Machine learning
Spatiotemporal distribution
Health impact assessment

ABSTRACT

Ambient fine particulate matter ($PM_{2.5}$) pollution is a major environmental and public health challenge in China. In the recent decade, the $PM_{2.5}$ level has decreased mainly driven by reductions in particulate sulfate as a result of large-scale desulfurization efforts in coal-fired power plants and industrial facilities. Emerging evidence also points to the differential toxicity of particulate sulfate affecting human health. However, estimating the long-term spatiotemporal trend of sulfate is difficult because a ground monitoring network of $PM_{2.5}$ constituents has not been established in China. Spaceborne sensors such as the Multi-angle Imaging SpectroRadiometer (MISR) instrument can provide complementary information on aerosol size and type. With the help of state-of-the-art machine learning techniques, we developed a sulfate prediction model under support from available ground measurements, MISR-retrieved aerosol microphysical properties, and atmospheric reanalysis data at a spatial resolution of 0.1° . Our sulfate model performed well with an out-of-bag cross-validation R^2 of 0.68 at the daily level and 0.93 at the monthly level. We found that the national mean population-weighted sulfate concentration was relatively stable before the Air Pollution Prevention and Control Action Plan was enforced in 2013, ranging from 10.4 to $11.5 \mu g m^{-3}$. But the sulfate level dramatically decreased to $7.7 \mu g m^{-3}$ in 2018, with a change rate of -28.7% from 2013 to 2018. Correspondingly, the annual mean total non-accidental and cardiopulmonary deaths attributed to sulfate decreased by 40.7% and 42.3% , respectively. The long-term, full-coverage sulfate level estimates will support future studies on evaluating air quality policies and understanding the adverse health effect of particulate sulfate.

1. Introduction

Fine particulate matter ($PM_{2.5}$, particulate matter with an aerodynamic diameter of less than $2.5 \mu m$) is a major air pollutant that has drawn concerns worldwide due to its adverse impacts on human health (Burnett et al. 2018b). Over the past three decades, China has

experienced severe $PM_{2.5}$ pollution from rapid economic development and urbanization that brought enormous public health burdens (Burnett et al. 2018b; Xue et al. 2019). Recently, a few studies have pointed out that the $PM_{2.5}$ level has significantly decreased mainly contributed by the decline of sulfate (SO_4^{2-}) concentration (Zhang and Geng 2019). Since 2005 and especially in 2013, the Chinese government implemented a

* Corresponding authors.

E-mail addresses: shixm@chinacdc.cn (X. Shi), yang.liu@emory.edu (Y. Liu).

¹ These authors contributed equally to this work.

series of air pollution control policies such as desulfurization, a chemical process to remove sulfur from coal-fired power plants and large industrial facilities. As a result, national mean sulfur dioxide (SO_2) emissions, the primary precursor of particulate sulfate, significantly decreased by 62 % from 2010 to 2017 (Zheng et al. 2018). Therefore, understanding the historical long-term spatiotemporal variation of sulfate in China will help evaluate the effectiveness of existing emission control policies and guide future regulations on improving air quality further.

$\text{PM}_{2.5}$ is a complex mixture of chemical constituents. The debate on which is the most toxic component of $\text{PM}_{2.5}$ is inconclusive; but, existing evidence indicates that the hazardous effects of long-term exposure to $\text{PM}_{2.5}$ constituents on population are differential. Previous studies found $\text{PM}_{2.5}$ constituents from fossil fuel combustion showed larger hazardous effects on mortality than those from natural sources (Chen et al. 2021; Crouse et al. 2016; Liang et al. 2022; Thurston et al. 2016). To compare the effect estimates regarding the same increment of pollution concentrations, some epidemiological studies found elemental or black carbon of $\text{PM}_{2.5}$ showed higher hazard (Liang et al. 2022; Ostro B. 2011). However, elemental carbon makes up a small percentage of total $\text{PM}_{2.5}$ mass concentrations and its concentration is much lower than secondary inorganic components (sulfate, nitrate, and ammonia). Therefore, if comparisons are based on the increment of inter-quartile range, some studies found that sulfate or sulfur has the strongest associations with mortality outcomes (Crouse et al. 2016; Ostro B. 2011; Thurston et al. 2016). Some previous cohort studies also have shown that effect estimates of long-term exposure to sulfate on mortality are higher than or at least comparable to that of total $\text{PM}_{2.5}$ exposure in terms of the same increment (Dockery et al. 1993; Krewski et al. 2009; Liang et al. 2022; Ostro B. 2011).

As one of the main $\text{PM}_{2.5}$ constituents in China, sulfate is likely associated with greater health risks than total $\text{PM}_{2.5}$. A few potential mechanisms have been proposed. First, the acidic sulfates could react with metals in $\text{PM}_{2.5}$, and convert insoluble and low toxicity metal oxides into metal ions that are soluble in the lung lining fluid and induce the production of highly reactive oxygenating compounds (Ghio et al. 1999; Rubasinghe et al. 2010; Schwartz and Lepeule 2012). Second, a recent study showed that sulfate ions could rapidly penetrate the lung surfactant barrier to the alveolar region, activate the cholesterol biosynthetic metabolism and induce the expression of genes related to tumorigenesis, which may help understand PM-related lung cancers (Park et al. 2022). Third, sulfate is reported to contribute to the formation of secondary organic particles and elemental carbon particles, for example, aiding the aging of freshly emitted soot particles and reacting with toluene and nitrogen oxides to form secondary organic particles (Popovicheva et al. 2011; Schwartz and Lepeule 2012; Wu et al. 2007).

Although sulfate is of potential toxicity and understanding its role in evaluating air quality policies is essential, the assessment of long-term sulfate exposure in China has been challenging due to the lack of a $\text{PM}_{2.5}$ speciation monitoring network (Huang et al. 2018). To date, large-scale estimation of sulfate levels mainly relies on chemical transport model (CTM) simulations that usually have large uncertainties from inaccurate emissions inventory and limited characterization of sulfate photochemical reactions (Fu et al. 2016; Geng et al. 2019; Xing et al. 2015). For example, the correlation coefficient (r) value between the Community Multiscale Air Quality (CMAQ) simulations and ground-based observations of monthly sulfate concentration over eastern China is only 0.53 (Geng et al. 2019). In addition, CTM-simulated sulfate estimates are largely driven by idealized model assumptions of SO_2 emissions, which confounds the goal of examining the actual impact of policy implementation.

Fortunately, machine learning models supported by large datasets of satellite remote sensing and atmospheric reanalysis have emerged as a powerful tool to estimate $\text{PM}_{2.5}$ constituents in developed countries (Di et al. 2016; Meng et al. 2018b). In addition, aerosol data retrieved by the Multiangle Imaging SpectroRadiometer (MISR) has been successfully

used to explain the daily variability of long-term sulfate concentration (Meng et al. 2018b). Hence, we developed a sulfate prediction model in China based on random forest algorithm, a machine learning model, driven by MISR-retrieved aerosol microphysical properties, available ground observations of sulfate concentration, and other supporting information from multiple large data sets. We then characterized the long-term spatiotemporal variation of sulfate in China from 2005 to 2018, and further evaluated the health benefit gained by the reduction in sulfate during this period.

2. Data and methods

2.1. Study design

Our study domain includes all provinces, autonomous regions, and special administrative regions of China (Fig. 1). A modeling grid with a spatial resolution of 0.1° was constructed for model development and health impact assessment across the entire domain. First, we built a random forest model to predict daily sulfate concentration. All data were either spatially averaged or interpolated by the inverse distance weighting (IDW) to match to modeling grid cells. The “out-of-bag” (OOB) bootstrap sampling strategy was used for predictor selection and model cross-validation (Meng et al. 2018b). Second, predicted daily sulfate concentrations were aggregated into monthly and annual means for investigating the spatiotemporal variations of sulfate in China from 2005 to 2018. In particular, we discussed the sulfate level of the four most populated city clusters in China, including the Beijing-Tianjin-Hebei (BTH) area in the North, Yangtze-River Delta (YRD) in the East, Cheng-Yu (CY) area in the West, and the Pearl River Delta (PRD) in the South, as outlined in Fig. 1. Finally, we calculated non-accidental and cardiovascular mortalities attributable to long-term sulfate exposure based on estimated sulfate exposure, pooled mortality risks of sulfate, age-specific population data in China, and the baseline mortality of specific outcomes.

2.2. Sulfate model development

2.2.1. Available ground observations

Approximately 21,000 daily measurements of ground sulfate concentration were collected from 88 monitoring sites across China from 2005 to 2018 (Fig. 1), including data from Hong Kong and Taiwan $\text{PM}_{2.5}$ speciation supersites (Huang et al. 2014; Lin et al. 2008). Compared with developed countries that have monitoring networks of $\text{PM}_{2.5}$ constituents, ground monitoring sites in China are limited. But observations of sulfate are relatively abundant that cover regions with different levels of population density (Fig. 1). Moreover, those sites are nearly evenly distributed in urban and rural areas of China (Hang et al. 2022). Although China does not have a uniform standard for measuring $\text{PM}_{2.5}$ constituents, a comparison study reported that sulfate measurements based on an online method combining Gas and Aerosol Collector (GAC) and Ion Chromatography (IC) were highly consistent with filter-based measurements, and the R^2 and slope of measurements from the two methods were 0.86 and 0.94, respectively (Dong et al. 2012). Therefore, we include all the available ground data in developing the prediction model to endure sufficient model training. Detailed information on each monitoring site used in this study is summarized in Table S1.

2.2.2. Unique MISR AOD

MISR aboard NASA's satellite Terra can measure solar radiance in four spectral bands at nine view angles that provides unique information on aerosol microphysical properties (Diner et al. 1998). Consequently, MISR's aerosol data products have been widely used to estimate the ground concentration of $\text{PM}_{2.5}$ constituents (Diner et al. 1998; Liu et al. 2007a; Liu et al. 2007b; Liu et al. 2011; Meng et al. 2018a). Here, we used the most recent Version 23 aerosol product of MISR Level 2 data with a spatial resolution of $4.4 \text{ km} \times 4.4 \text{ km}$ (Garay et al. 2020). It

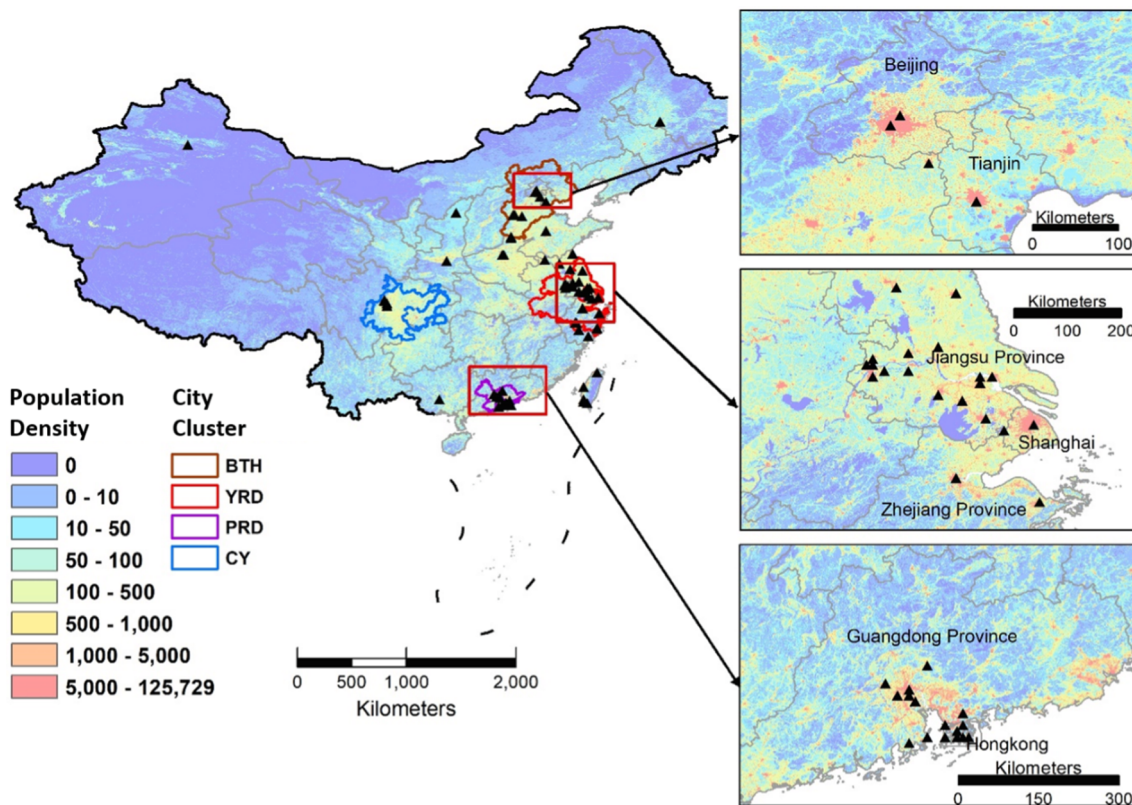


Fig. 1. Study domain and locations of available sulfate monitoring sites (black triangle) in China that were included in this study. The background of this map is colored by population density (people/km²) derived from LandScan population data for the year 2018.

reports fractional aerosol optical depth (AOD) retrievals of eight types of aerosol components (i.e., components #1, #2, #3, #6, #8, #14, #19, #21) defined by aerosol size, shape, refraction index, and scale height (Garay et al. 2017; Liu et al. 2009). A detailed description of those components is documented in Liu et al. (2007a). According to the microphysical property of sulfate, non-absorption AOD components (i.e., #2 and #3), small mode AOD (particle radius smaller than 0.35 μm), and medium mode AOD (particle radius ranges from 0.35 to 0.7 μm) were selected as predictors to develop the sulfate model. The method of calculating AOD components with 74 aerosol mixtures of MISR retrieval is documented in Liu et al. (2007a). In this study, we integrated annual mean AOD data into the prediction model as MISR's swath is relatively narrow.

2.2.3. Other supporting data

To boost the model's performance, we considered the influence of atmospheric visibility, atmospheric components, meteorological conditions, land cover, and population density on sulfate prediction. Ground-level daily visibility data were extracted from the Integrated Surface Dataset (IDS) from the U.S. National Oceanic and Atmospheric Administration (NOAA) National Centers for Environmental Information (NCEI). Additionally, we included monthly mean cloud cover data at 1° × 1° resolution downloaded from Clouds and the Earth's Radiant Energy System (CERES) cloud product that provides the best estimate of clouds from seven polar-orbiting and geostationary instruments (Wielicki et al. 1998). Daily SO₂ at 0.75° × 0.75 spatial resolution was extracted from the Copernicus Atmosphere Monitoring Service (CAMS) reanalysis (Inness et al. 2019). Daily simulated sulfate concentration at 0.5° × 0.625° resolution was obtained from the Modern-Era Retrospective Analysis for Research and Applications model (MERRA-2) (Randles et al. 2017). Monthly mean Normalized Difference Vegetation Index (NDVI) was calculated using the MODIS NDVI product (MOD13A3) at 1 km resolution. Daily meteorological data of

temperature at 2-meter, humidity at 2-meter, and the planetary boundary layer height (PBLH) were downloaded from the Goddard Earth Observing System Model at a resolution of 0.5° × 0.625° (2005–2012) and a resolution of 0.25° × 0.3125° (2013–2018). Annual population data were obtained from the LandScan Global Population Database at about 1 km resolution (Dobson et al. 2000) and summed within the study grid.

2.2.4. Modeling method

A random forest model was trained by about 21,000 records of ground observations to estimate daily sulfate concentrations in China. We set 1000 decision trees in the forest based on the balance of prediction accuracy and computing time. We consider 14 features by each tree when splitting a node by testing different sets of predictors. The OOB bootstrap sampling strategy was used to develop the model (Liaw and Wiener 2002). One unique strength of the random forest algorithm is that it can rank the importance of each predictor by comparing normalized mean errors (MSE) between predictions before and after that variable is permuted while all others are left unchanged. Therefore, the model performance was tested by calculating MSE and R² values between observations and predictions. The final predictors include visibility, SO₂, simulated sulfate concentrations, MISR fractional AODs, population density, PBLH, temperature, humidity, NDVI, cloud cover, and month (Figure S1). In addition to calculating OOB cross validations (CVs), we conducted random CVs to further test the model's capacity of predicting accuracy where ground observations were unavailable (Figure S2). In the test, ground sulfate observations were divided into groups and sulfate predictions were generated by a random forest model trained with data elsewhere.

2.3. Mortality burden of sulfate

2.3.1. meta-analysis of mortality risks

Mortality risk estimates for long-term sulfate exposure in China do not exist. Therefore, we assume the toxicity of sulfate is constant across the range of exposure levels and conducted a *meta*-analysis to pool the relative risk (RR) of sulfate from published cohort studies that: 1) reported numeric associations between long-term exposure to sulfate and mortality, and 2) documented explicit increments of sulfate concentrations corresponding to the risk estimates. Studies derived from the same cohort but during different follow-up periods with distinct exposure assessments were considered independent. As a result, we selected five studies that estimated RRs for sulfate-related total non-accidental and cardiopulmonary mortalities (Table 1). Those studies were extracted from three cohorts conducted in the United States (US), including California Teachers Study (CTS), Harvard Six Cities Study, and American Cancer Society (ACS) Cohort with sulfate levels ranging from 0.62 to 23.5 $\mu\text{g m}^{-3}$ (Dockery et al. 1993; Krewski et al. 2009; Ostro B. 2011; Pope et al. 1995). We made a reasonable assumption that the RR estimate exhibits a log-linear shape because the Global Exposure Mortality Model (GEMM) shows a near-linear shape of lnRR at high PM_{2.5} levels (Burnett et al. 2018). Additionally, a recent study based on the Chinese census data suggested that census-based deaths attributable to PM_{2.5} were in better agreement with results from the GEMM than the Integrated Exposure-Response (IER) model (Xue et al. 2019). The mortality RR from different studies was first unified corresponding to a 1 $\mu\text{g m}^{-3}$ increment then pooled through *meta*-analysis based on the random effects model.

2.3.2. Population and mortality data

We downloaded gridded population counts by age in 2010 from Basic Demographic Characteristics (Revision 11) of the Gridded Population of the World Version 4 (GPWv4) with 2.5 arc-minute spatial resolution (<https://sedac.ciesin.columbia.edu>). The age-specific population data in each 5-year age group were used to calculate the ratios of the age-specific population in the total population. Because the age structure data are only available for 2010, we assumed that the population pyramids were the same during the study period. Then, the age-specific population counts for each year were calculated based on the age-specific ratios from GPW and the LandScan population data. Cause-specific mortality data for each 5-year age group for urban and rural areas were obtained from the Chinese National Health Statistics Yearbooks, and the ratio of urban and rural population to the total

population for each year at the country level was obtained from the National Bureau of Statistics of China. Finally, disease-specific death counts by age from 2005 to 2018 were calculated for each grid cell.

2.3.3. Calculation of the mortality burden

We first calculated national-level population attributable fraction (PAF) with gridded population data, following Equations (1)-(3) (Cohen et al. 2017):

$$RR_i = e^{\beta(x_i - x_{cf})} \quad (1)$$

$$paf_i = \frac{RR_i - 1}{RR_i} \quad (2)$$

$$PAF = 1 - \frac{\sum_{i=1}^{n_{grid}} POP_i * (1/(1-paf_i))}{\sum_{i=1}^{n_{grid}} POP_i} \quad (3)$$

where β is the pooled health effect; x_i is the estimated sulfate concentration in grid cell i ; x_{cf} is the counterfactual concentration calculated as the average value of minimum sulfate concentrations reported in studies included in the *meta*-analysis (2.5 $\mu\text{g m}^{-3}$); POP_i is the population and paf_i is the PAF of the specific outcome in grid cell i . Because all the studies included in our *meta*-analysis were conducted with adult participants, we only considered a population older than 25 years of age in our calculations. Next, the attributable death (AD) was calculated using Equation (4) for total non-accidental and cardiopulmonary mortalities, respectively:

$$AD = PAF \times POP \times Mortality \quad (4)$$

Where the AD was calculated for each age group first and then summed for all populations older than 25 years old.

3. Results

3.1. Model performance in estimating sulfate in China

In total, 21,000 ground observations of sulfate from 88 monitoring sites were included in model development. Our sulfate prediction model was developed with 14 predictors as listed in Figure S1 ranked by permutation feature importance. Nearly half of those predictors are retrieved by satellite instruments (i.e., AOD, NDVI, cloud cover) and MISR data made a major contribution to the model despite its modest temporal resolution. Fig. 2 shows the linear regression and scatter plot

Table 1

Summary of cohort studies that reported relative risks of long-term exposure to sulfate for total non-accidental mortality (RR_{Total}) and cardiopulmonary mortality (RR_{CP}).

Cohort	Sulfate increment ($\mu\text{g/m}^{-3}$ (-))	RR _{Total} (95 % CI)	RR _{CP} (95 % CI)	Exposure level	Sulfate range ($\mu\text{g/m}^{-3}$ (-))	Reference
Harvard Six Cities Study (1979–1989)	8.0	1.26 (1.08–1.47)	–	Community level	4.8–12.8	(Dockery et al. 1993)
ACS Cohort (1982–1989)	19.9	1.15 (1.09–1.22)	1.26 (1.16–1.37)	Metropolitan Statistical Areas	3.6–23.5	(Pope et al. 1995)
ACS Cohort extended follow-up (1982–2000)	5.0	1.045 (1.034–1.056)	1.054 (1.038–1.071)	Metropolitan Areas, 1980–1981	1.4–15.64	(Krewski et al. 2009)
ACS Cohort extended follow-up (1982–2000)	5.0	1.086 (1.060–1.113)	1.114 (1.074–1.156)	Metropolitan Areas, 1990	1.96–10.65	(Krewski et al. 2009)
California Teachers Study (2002–2007)	2.2	1.06 (0.97–1.16)	1.14 (1.01–1.29)	Based on residential addresses	0.62–7.4	(Ostro B. 2011)

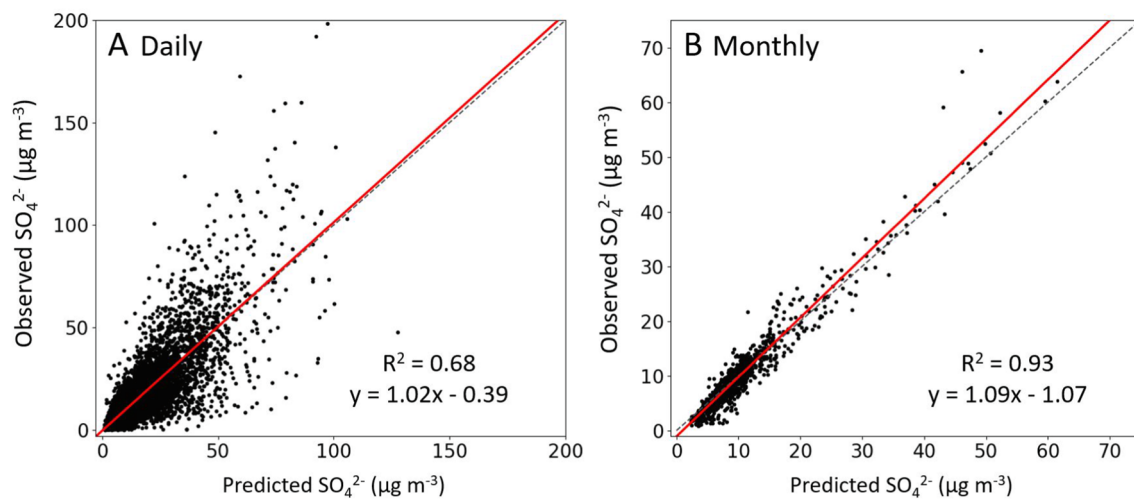


Fig. 2. Linear regression between measured and OOB predicted sulfate concentrations of the sulfate model at the (A) daily and (B) monthly levels. The black dashed line is the 1:1 line. The red line is the regression line. (For interpretation of the references to colour in this figure legend, the reader is referred to the web version of this article.)

between observed and predicted sulfate concentrations at daily and monthly levels. The monthly means were calculated if more than seven daily observations were available for a given monitoring site and month. Predicted sulfate concentrations agree well with ground observations as the slope of regression lines is close to unity and intercepts are close to zero. The model's OOB CV R^2 value of daily and monthly mean sulfate concentrations is 0.68 and 0.93, respectively, indicating little prediction bias. We further conducted a random CV of the model to test the model's reliability and stability (Figure S2). Time-series comparisons between measured and predicted sulfate concentrations demonstrate that our model can capture the temporal variability of ground sulfate at six monitoring sites in different geographical regions of China (Fig. 3). Before 2013, only a few ground sites in China can monitor sulfate levels. Our model is able to predict both high and low concentrations of sulfate

during the period (Fig. 3A-B). Since 2013, limited minor sites have been built in populated megacities such as Beijing, Shanghai, and Chengdu. Our model can capture extreme pollution events and seasonal variations of sulfate over those places (Fig. 3C-F). Interestingly, different from previous studies reporting that $\text{PM}_{2.5}$ concentrations in China generally peaked in 2013, the level of sulfate in Chengdu was extremely high in 2014 with a concentration of approximately $70 \mu\text{g m}^{-3}$ (Fig. 3E). In Beijing, the sulfate level in 2014 was even higher than that of 2013 according to ground observations (Fig. 3D).

Based on the newly built exposure model, we estimated the spatial and temporal trends of sulfate concentrations in China from 2005 to 2018. We found that population-weighted national annual mean sulfate was relatively stable before 2013 with a range of $10.4\text{--}11.5 \mu\text{g m}^{-3}$, but significantly decreased to $7.7 \mu\text{g m}^{-3}$ in 2018 (Figure S3). Among the

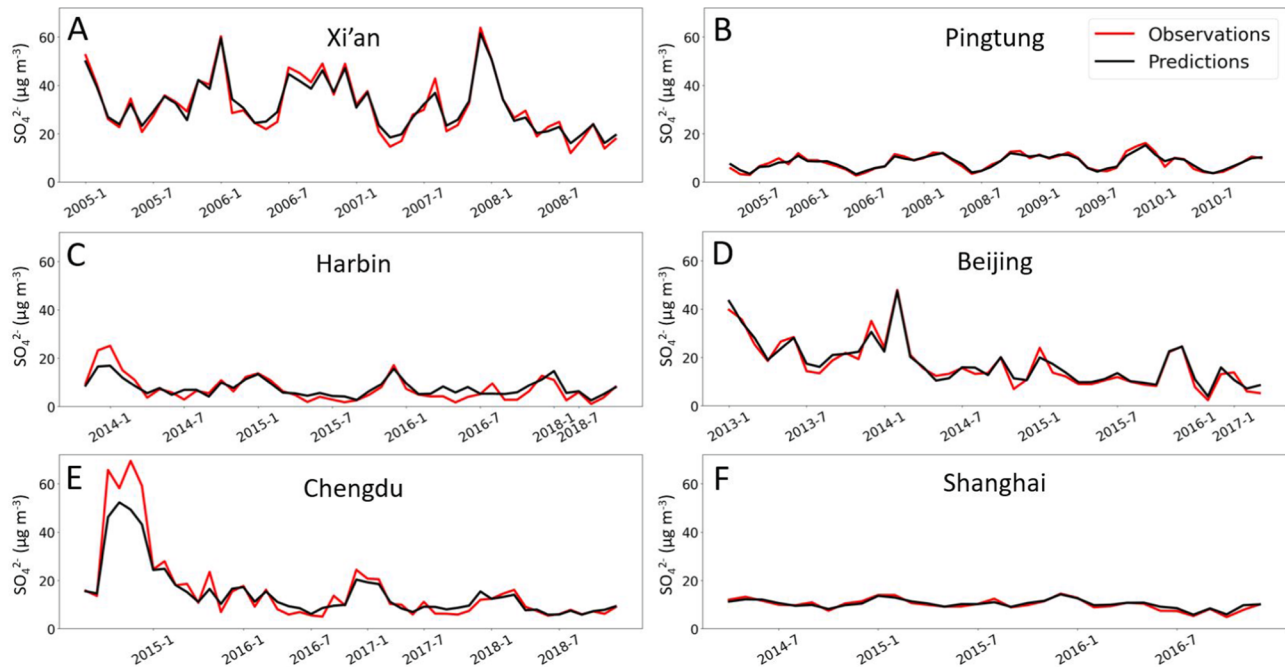


Fig. 3. Predicted (black line) and observed (red line) monthly mean sulfate concentrations at six monitoring sites of different geographical regions in China: (A) Xi'an in the Northwest, (B) Pingtung in the South, (C) Harbin in the Northeast, (D) Beijing in the North, (E) Chengdu in the West, and (F) Shanghai in the East. (For interpretation of the references to colour in this figure legend, the reader is referred to the web version of this article.)

four city clusters, BTH and CY were used to experience the worst pollution with an annual mean sulfate concentration of around $15 \mu\text{g m}^{-3}$. However, the regional disparities substantially shrank in 2018 and resulted in a similar sulfate level of approximately $8 \mu\text{g m}^{-3}$ over those clusters. Fig. 4 shows the spatial distributions of the annual mean sulfate concentration in China in the first (2005) and last (2018) year of our study period and the year when the Air Pollution Prevention and Control Action Plan was implemented (2013). Spatially, the highest sulfate level was found in the CY and BTH regions with mean sulfate concentrations of more than $20 \mu\text{g m}^{-3}$ in 2005 and 2013, and decreased to less than $10 \mu\text{g m}^{-3}$ in 2018. The lowest levels occurred over the Tibetan Plateau with mean concentrations of about $5 \mu\text{g m}^{-3}$ during the study period.

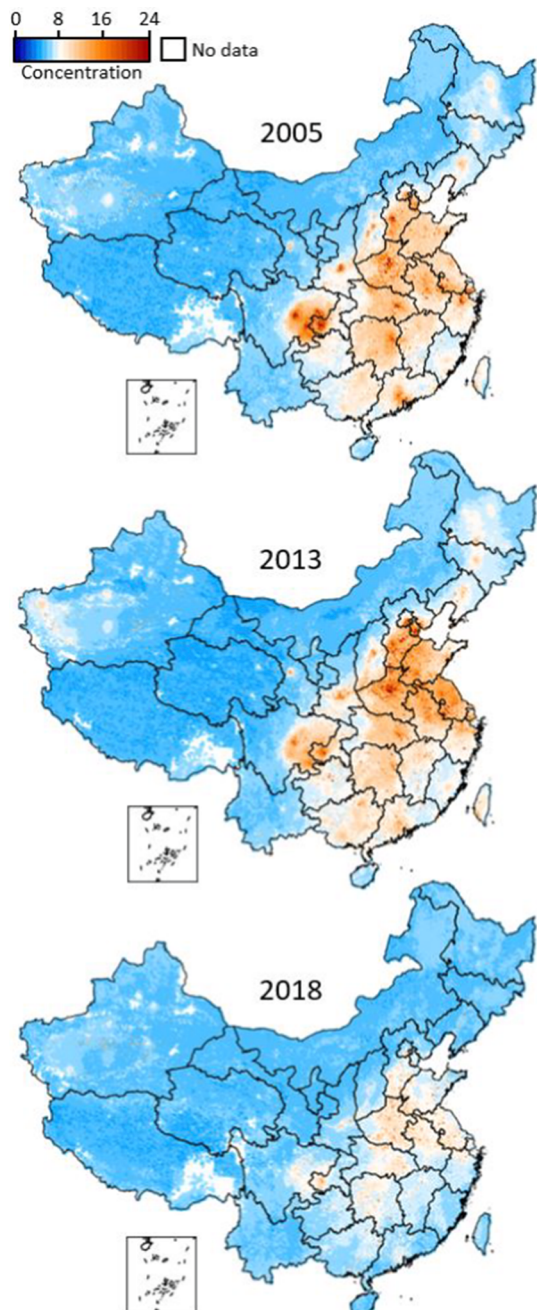


Fig. 4. Spatial distributions of annual mean sulfate predictions ($\mu\text{g}/\text{m}^3(-|-)$) in China in 2005, 2013, and 2018. The missing values shown as no data were caused by data missingness of MISR AOD components.

3.2. Mortality burden attributable to long-term sulfate exposure

Table 1 summarizes studies used to pool the RR estimate of total non-accidental mortality (RR_{Total}) and cardiopulmonary mortality (RR_{CP}) attributable to long-term sulfate air pollution, including the Harvard Six Cities Study, American Cancer Society (ACS) cohort, and the California Teachers Study. Note that we pooled three results from the ACS cohort, one is the original analysis with a period of 1982–1989, and the other two were ACS extended follow-up analyses during 1982–2000 with different exposure assessments. The β value from the meta-analysis for total non-accidental mortality was 0.0103 with a 95 % confidential interval of 0.0074 – 0.0132 corresponding to a $1 \mu\text{g m}^{-3}$ increment in sulfate concentration at annual level. The β value for cardiopulmonary mortality was 0.0145 (95 % CI: 0.0079 – 0.0212) for a $1 \mu\text{g m}^{-3}$ increment in sulfate. **Table 2** compares the national annual mean population-weighted sulfate levels with estimated total non-accidental and cardiopulmonary deaths in the three selected years. A decline was observed in the mortality burden attributable to sulfate from 2005 to 2013 despite the sulfate concentrations slightly increased. This is because the total number of non-accidental deaths in China decreased from 8089 thousands in 2005 to 6840 thousands in 2013 as reported by the National Bureau of Statistics of China (<http://data.stats.gov.cn/>). From 2013 to 2018, as sulfate concentrations dropped by 28.7 %, the total non-accidental deaths (AD_{Total}) and the cardiopulmonary deaths (AD_{CP}) attributable to sulfate exposure significantly decreased by 40.7 % and 42.3 %, respectively.

4. Discussion

This study is the first attempt to estimate long-term particulate sulfate concentrations across China with satellite-driven machine learning models trained by ground measurements. Although the size of the training dataset is relatively small due to limited available monitoring sites of $\text{PM}_{2.5}$ constituents in China, our model achieved stronger performance than classical CTMs. For example, CMAQ-simulated $\text{PM}_{2.5}$ constituents were constrained with satellite-based $\text{PM}_{2.5}$ estimations in predicting sulfate in eastern China from 2013 to 2017 (Geng et al. 2019). This method can help enhance the correlation coefficient between modeled and measured sulfate concentrations from 0.53 (CMAQ simulations only) to 0.60 (constrained CMAQ simulations). Compared with Geng et al. (2019), the R^2 value of our model is significantly higher at 0.68 with an extended study period (2005–2018) and full national coverage. The improvement is attributed to two main factors. First, we used the random forest algorithm that makes few assumptions on the independence of the measurements and the distribution of the predictors, which allows better capture of the nonlinear associations

Table 2

Population-weighted sulfate concentrations (SO_4^{2-}), total non-accidental mortality (AD_{Total}) and cardiopulmonary mortality (AD_{CP}) attributable to sulfate pollution in China in 2005, 2013, and 2018 among the population with age over 25.

Year	SO_4^{2-} ($\mu\text{g}/\text{m}^3(- -)$)	AD_{Total} in thousands (95 % CI)	AD_{CP} in thousands (95 % CI)
2005	10.5	656 (476–832)	586 (326–837)
2013	10.9	582 (423–739)	501 (279–715)
2018	7.8	345 (250–440)	289 (160–416)
Change rate (2013–2005)/ 2005	+3.6 %	-11.3 %	-14.5 %
Change rate (2018–2013)/ 2013	-28.7 %	-40.7 %	-42.3 %

between the sulfate concentrations and model predictors. Second, our model was trained by ground measurements, satellite observations of aerosol, cloud, land cover, and atmospheric reanalysis of meteorological conditions, atmospheric composition to provide complementary spatiotemporal information for predicting sulfate concentrations over complex land surfaces (Figure S1). In particular, MISR fractional AODs provide the model with unique information on particle size, shape, and light absorption to help characterize the spatial patterns and long-term trends of sulfate.

With the help of the newly-developed high-performance model, we found that existing air quality control policies were effective in decreasing sulfate concentrations. For example, the 11th and 12th Five Year Plans initiated in 2006 and 2011 respectively successfully limited sulfate through the desulphurization of rapidly growing coal-fired power plants and industrial sectors. Then, the toughest-ever Air Pollution Prevention and Control Action Plan (APPCAP) released in 2013 further reduced SO₂ emissions by about 60 % (Zheng et al. 2018). Our calculations show that population-weighted annual mean sulfate concentrations decreased by 28.7 % in China from 2013 to 2018. This decline is consistent with previous studies and demonstrates that the construction of desulphurization facilities successfully reduced sulfate without jeopardizing rapid economic development, providing a reference for other developing countries trying to control PM_{2.5} pollution (Geng et al. 2019; Yuan et al. 2013; Zhao et al. 2021). The spatial patterns of sulfate concentrations in China have changed over time, though sulfate levels in eastern China remain higher than those in the western regions. Major city clusters suffered severe sulfate pollution especially until the birth of APPCAP, which required PM_{2.5} concentrations to decrease by 25 %, 20 %, and 15 % in the BTH, YRD, and PRD regions from 2013 to 2017, respectively. As a result, APPCAP powerfully promoted the decrease of total PM_{2.5} as well as sulfate concentrations in these key regions. The gap in sulfate concentrations between these city clusters and other parts of China was closed in 2018, when the average sulfate concentrations fell to approximately 10 µg m⁻³ in eastern China. Those findings suggest that emissions reduction policies could be extended from key city clusters to surrounding areas to further decrease sulfate concentrations and improve air quality.

Combining predicted long-term sulfate concentrations, baseline mortality data, and pooled risk estimates, we find that the total non-accidental death attributed to sulfate exposure decreased by 40.7 % from 582 thousands in 2013 to 345 thousands in 2018; while the total non-accidental mortality decreased by only 6.4 % during the same period. Compared with previous studies that evaluated the excess deaths attributable to total PM_{2.5}, long-term exposure to sulfate likely exhibits a higher health risk (Table S2). For example, it is estimated that a 33 % decrease in PM_{2.5} concentrations led to 13.1 % (54.92 thousand) fewer deaths in 74 key Chinese cities from 2013 to 2017 based on IER functions (Huang et al. 2018). In our study, a lower decrease (28.7 %) in sulfate concentrations results in a much higher drop (40.7 %) in total non-accidental deaths attributable to sulfate concentrations from 2013 to 2018 because of higher population density in regions with higher sulfate pollution, indicating the decrease in sulfate played a significant role in the decline of deaths attributable to total PM_{2.5} especially in populated areas. But note that the IER study estimated the shape of log-transformed RR of non-accidental death from PM_{2.5} exposure flattens at higher PM_{2.5} concentrations; however, we assumed a linear lnRR shape for sulfate exposure. As different methods of calculating the exposure-response coefficients may bring large disparities in estimating the reduction magnitude of air pollutants, we further compared the sulfate health burden with GEMM-based studies. Burnett et al. (2018a) reported 2,470 thousand excess non-accidental deaths (including dominant causes such as noncommunicable diseases (NCD) and lower respiratory infections (LRIs)) in China in 2015, when the population-weighted PM_{2.5} level was 57.5 µg m⁻³. Liang et al. (2020) estimated that the annual mortality burden due to PM_{2.5} exposure decreased by 18.2 % (from 2.2 million to 1.8 million) with national mean PM_{2.5}

concentrations decreasing by 11 % (from 47.0 µg m⁻³ to 41.5 µg m⁻³) from 2013 to 2016. Compared to our result of 582 thousand excess deaths at sulfate levels of 10.9 µg m⁻³ in 2013, the ratio of excess deaths attributable to sulfate concentrations and total PM_{2.5} (0.19) is close to but slightly higher than the ratio of sulfate to PM_{2.5} concentrations (0.24) because of higher effect estimates of sulfate than total PM_{2.5}.

5. Limitations

Our study has a few limitations. First, the number of ground sulfate measurements used for model training was smaller than the datasets used to develop national-scale PM_{2.5} total mass models. The limited number of monitoring stations might also introduce uncertainties when predicting sulfate in areas and during the period with few sulfate measurements. Many stations measured sulfate discontinuously, which might miss the extremely high pollution episodes and cause underestimations in the predictions. As more speciation monitors become available in China, we will retrain our model to improve its performance. Moreover, MISR has a narrow swath that leads to limited spatial coverage for the exposure estimates. As indicated in Fig. 4, sulfate predictions are not available over eastern Tibet (colored in white). Gap-filling approaches are required for future studies to fill missing AOD retrievals to improve the model's spatial coverage. Second, only a few studies to date have reported the mortality RRs of long-term exposure to particulate sulfate, all of which were conducted in developed countries with lower sulfate concentrations, different demographics and socio-economic characteristics. Therefore, the pooled RR may not fully represent the adverse health effects of sulfate in China. We will reassess the health risk when a cohort study of sulfate in China is available. Third, we used the age structure in 2010 for all years due to a lack of accurate estimates for other years. Due to China's aging population, this assumption may lead to an underestimation of the attributable deaths after 2010. Fourth, we did not fit the exposure-response curve between long-term sulfate exposure and mortality; instead, we pooled the effect estimates based on several studies. We assumed the association between sulfate concentrations and lnRR as linear, which may overestimate the attributable deaths if their association tends to flatten at higher pollution levels as for total PM_{2.5} mass concentration. So far, only limited cohort studies have investigated the association between sulfate and mortality. We will develop the E-R curve when more data are available in the future.

6. Conclusion

We reported a high-performance machine learning model to predict particulate sulfate concentrations at a 0.1° resolution across the entire China from 2005 to 2018. Our results showed a marked decline in sulfate levels during the past 14 years as a result of effective emission control policies and the corresponding large health benefits due to better air quality. Given the scarcity of PM_{2.5} speciation measurements, those long-term sulfate estimates will enable environmental epidemiological studies on the exposure to major PM_{2.5} constituents in China, and benefit the understanding of global excess mortality from ambient air pollution.

CRediT authorship contribution statement

Xia Meng: Methodology, Software, Formal analysis, Data curation, Investigation, Writing – original draft, Writing – review & editing, Visualization. **Yun Hang:** Methodology, Software, Formal analysis, Data curation, Investigation, Writing – original draft, Writing – review & editing, Visualization. **Xiuran Lin:** Resources, Writing – review & editing. **Tiantian Li:** Resources, Writing – review & editing. **Tijian Wang:** Resources, Writing – review & editing. **Junji Cao:** Resources, Writing – review & editing. **Qingyan Fu:** Resources, Writing – review & editing. **Sagnik Dey:** Resources, Writing – review & editing. **Kan Huang:** Resources, Writing – review & editing. **Fengchao Liang:**

Resources, Writing – review & editing. **Haidong Kan:** Resources, Writing – review & editing. **Xiaoming Shi:** Resources, Writing – review & editing. **Yang Liu:** Conceptualization, Methodology, Resources, Writing – review & editing, Supervision, Funding acquisition.

Declaration of Competing Interest

The authors declare that they have no known competing financial interests or personal relationships that could have appeared to influence the work reported in this paper.

Data availability

Data will be made available on request.

Acknowledgment

This work was supported by the National Institute of Environmental Health Sciences (NIEHS) of the National Institutes of Health (Award # 1R01ES032140). The content is solely the responsibility of the authors and does not necessarily represent the official views of NIEHS.

Appendix A. Supplementary data

Supplementary data to this article can be found online at <https://doi.org/10.1016/j.envint.2023.107740>.

References

- Burnett, R., Chen, H., Szyszkowicz, M., Fann, N., Hubbell, B., Pope, C.A., Apte, J.S., Brauer, M., Cohen, A., Weichenthal, S., Coggins, J., Di, Q., Brunekreef, B., Frostad, J., Lim, S.S., Kan, H.D., Walker, K.D., Thurston, G.D., Hayes, R.B., Lim, C.C., Turner, M.C., Jerrett, M., Krewski, D., Gapstur, S.M., Diver, W.R., Ostro, B., Goldberg, D., Crouse, D.L., Martin, R.V., Peters, P., Pinault, L., Tjeenkema, M., Donkelaar, A., Villeneuve, P.J., Miller, A.B., Yin, P., Zhou, M.G., Wang, L.J., Janssen, N.A.H., Marra, M., Atkinson, R.W., Tsang, H., Thach, Q., Cannon, J.B., Allen, R.T., Hart, J.E., Laden, F., Cesaroni, G., Forastiere, F., Weinmayr, G., Jaensch, A., Nagel, G., Concin, H., Spadaro, J.V., 2018. Global estimates of mortality associated with long-term exposure to outdoor fine particulate matter. *P Natl Acad Sci USA* 115, 9592–9597.
- Burnett, R.; Chen, H.; Szyszkowicz, M.; Fann, N.; Hubbell, B.; Pope, C.A.; Apte, J.S.; Brauer, M.; Cohen, A.; Weichenthal, S. Global estimates of mortality associated with long-term exposure to outdoor fine particulate matter. *Proceedings of the National Academy of Sciences* 2018a;115:9592-9597.
- Chen, Y.; Chen, R.; Chen, Y.; Dong, X.; Zhu, J.; Liu, C.; van Donkelaar, A.; Martin, R.V.; Li, H.; Kan, H. The prospective effects of long-term exposure to ambient PM_{2.5} and constituents on mortality in rural East China. *Chemosphere* 2021;280:130740.
- Cohen, A.J., Brauer, M., Burnett, R., Anderson, H.R., Frostad, J., Estep, K., Balakrishnan, K., Brunekreef, B., Dandona, L., Dandona, R., Feigin, V., Freedman, G., Hubbell, B., Jobling, A., Kan, H., Knibbs, L., Liu, Y., Martin, R., Morawska, L., Pope, C.A., Shin, H., Straif, K., Shaddick, G., Thomas, M., van Dingen, R., van Donkelaar, A., Vos, T., Murray, C.J.L., Forouzanfar, M.H., 2017. Estimates and 25-year trends of the global burden of disease attributable to ambient air pollution: an analysis of data from the Global Burden of Diseases Study 2015. *Lancet* 389, 1907–1918.
- Crouse, D.L., Philip, S., Van Donkelaar, A., Martin, R.V., Jessiman, B., Peters, P.A., Weichenthal, S., Brook, J.R., Hubbell, B., Burnett, R.T., 2016. A new method to jointly estimate the mortality risk of long-term exposure to fine particulate matter and its components. *Scientific reports* 6, 1–10.
- Di, Q., Koutrakis, P., Schwartz, J., 2016. A hybrid prediction model for PM_{2.5} mass and components using a chemical transport model and land use regression. *Atmos Environ* 131, 390–399.
- Diner, D.J., Beckert, J.C., Reilly, T.H., Bruegge, C.J., Conel, J.E., Kahn, R.A., Martonchik, J.V., Ackerman, T.P., Davies, R., Gerstl, S.A., 1998. Multi-angle Imaging SpectroRadiometer (MISR) instrument description and experiment overview. *IEEE Transactions on Geoscience and Remote Sensing* 36, 1072–1087.
- Dobson, J.E., Bright, E.A., Coleman, P.R., Durfee, R.C., Worley, B.A., 2000. LandScan: A global population database for estimating populations at risk. *Photogramm Eng Rem S* 66, 849–857.
- Dockery, D.W.; Pope, C.A., 3rd; Xu, X.; Spengler, J.D.; Ware, J.H.; Fay, M.E.; Ferris, B.G., Jr.; Speizer, F.E. An association between air pollution and mortality in six U.S. cities. *N Engl J Med* 1993;329:1753-1759.
- Dong, H., Zeng, L., Hu, M., Wu, Y., Zhang, Y., Slanina, J., Zheng, M., Wang, Z., Jansen, R., 2012. The application of an improved gas and aerosol collector for ambient air pollutants in China. *Atmospheric Chemistry and Physics* 12, 10519.
- Fu, X., Wang, S.X., Chang, X., Cai, S.Y., Xing, J., Hao, J.M., 2016. Modeling analysis of secondary inorganic aerosols over China: pollution characteristics, and meteorological and dust impacts. *Sci Rep-Uk* 6, 35992.
- Garay, M.J., Kalashnikova, O.V., Bull, M.A., 2017. Development and assessment of a higher-spatial-resolution (4.4 km) MISR aerosol optical depth product using AERONET-DRAGON data. *Atmos. Chem Phys* 17, 5095–5106.
- Garay, M.J., Witek, M.L., Kahn, R.A., Seidel, F.C., Limbacher, J.A., Bull, M.A., Diner, D.J., Hansen, E.G., Kalashnikova, O.V., Lee, H., 2020. Introducing the 4.4 km spatial resolution Multi-Angle Imaging SpectroRadiometer (MISR) aerosol product. *Atmospheric Measurement Techniques* 13, 593–628.
- Geng, G., Xiao, Q., Zheng, Y., Tong, D., Zhang, Y., Zhang, X., Zhang, Q., He, K., Liu, Y., 2019. Impact of China's Air Pollution Prevention and Control Action Plan on PM 2.5 chemical composition over eastern China. *Science China Earth Sciences* 1–13.
- Ghio, A.J., Stoneheurner, J., McGee, J.K., Kinsey, J.S., 1999. Sulfate content correlates with iron concentrations in ambient air pollution particles. *Inhalation toxicology* 11, 293–307.
- Hang, Y.; Meng, X.; Li, T.; Wang, T.; Cao, J.; Fu, Q.; Dey, S.; Li, S.; Huang, K.; Liang, F. Assessment of long-term particulate nitrate air pollution and its health risk in China. *iScience* 2022:104899.
- Huang, X.H., Bian, Q., Ng, W.M., Louie, P.K., Yu, J.Z., 2014. Characterization of PM_{2.5} major components and source investigation in suburban Hong Kong: a one year monitoring study. *Aerosol and Air Quality Research* 14, 237–250.
- Huang, J., Pan, X.; Guo, X.; Li, G. Health impact of China's Air Pollution Prevention and Control Action Plan: an analysis of national air quality monitoring and mortality data. *The Lancet Planetary Health* 2018;2:e313-e323.
- Inness, A., Ades, M., Agusti-Panareda, A., Barré, J., Benedictow, A., Blechschmidt, A.-M., Dominguez, J.J., Engelen, R., Eskes, H., Flemming, J., 2019. The CAMS reanalysis of atmospheric composition. *Atmospheric Chemistry and Physics* 19, 3515–3556.
- Krewski, D., Jerrett, M., Burnett, R.T., Ma, R., Hughes, E., Shi, Y., Turner, M.C., Pope, C. A., 3rd; Thurston, G., Calle, E.E., Thun, M.J., Beckerman, B., DeLuca, P., Finkelstein, N., Ito, K., Moore, D.K., Newbold, K.B., Ramsay, T., Ross, Z., Shin, H., Tempalski, B. Extended follow-up and spatial analysis of the American Cancer Society study linking particulate air pollution and mortality. *Res Rep Health Eff Inst* 2009;5:114; discussion 115-136.
- Liang, R., Chen, R., Yin, P., van Donkelaar, A., Martin, R.V., Burnett, R., Cohen, A.J., Brauer, M., Liu, C., Wang, W., 2022. Associations of long-term exposure to fine particulate matter and its constituents with cardiovascular mortality: A prospective cohort study in China. *Environment International* 162, 107156.
- Liang, F.C., Xiao, Q.Y., Huang, K.Y., Yang, X.L., Liu, F.C., Li, J.X., Lu, X.F., Liu, Y., Gu, D. F., 2020. The 17-y spatiotemporal trend of PM_{2.5} and its mortality burden in China. *P Natl Acad Sci USA* 117, 25601–25608.
- Liaw, A., Wiener, M., 2002. Classification and regression by randomForest. *R news* 2, 18–22.
- Lin, C.-H., Wu, Y.-L., Lai, C.-H., Watson, J.G., Chow, J.C., 2008. Air quality measurements from the southern particulate matter supersite in Taiwan. *Aerosol and Air Quality Research* 8, 233–264.
- Liu, Y., Kahn, R., Kourtrakis, P., 2007a. Estimating PM_{2.5} component concentrations and size distributions using satellite retrieved fractional aerosol optical depth: part I - method development. *J Air & Waste Manage Assoc* 57, 1351–1359.
- Liu, Y., Kahn, R., Turquety, S., Yantoscia, R.M., Kourtrakis, P., 2007b. Estimating PM_{2.5} Component Concentrations and Size Distributions Using Satellite Retrieved Fractional Aerosol Optical Depth: Part II - A Case Study. *J Air & Waste Manage Assoc* 57, 1360–1369.
- Liu, Y., Schichtel, B.A., Kourtrakis, P., 2009. Estimating Particle Sulfate Concentrations Using MISR Retrieved Aerosol Properties. *Ieee J-Stars* 2, 176–184.
- Liu, Y., Wang, Z.F., Wang, J., Ferrare, R.A., Newsom, R.K., Welton, E.J., 2011. The effect of aerosol vertical profiles on satellite-estimated surface particle sulfate concentrations. *Remote Sens Environ* 115, 508–513.
- Meng, X.; Hand, J.L.; Schichtel, B.A.; Liu, Y. Space-time trends of PM_{2.5} constituents in the conterminous United States estimated by a machine learning approach, 2005–2015. *Environment International* 2018b;121:1137-1147.
- Meng, X., Garay, M.J., Diner, D.J., Kalashnikova, O.V., Xu, J., Liu, Y., 2018a. Estimating PM_{2.5} speciation concentrations using prototype 4.4 km-resolution MISR aerosol properties over Southern California. *Atmospheric Environment* 181, 70–81.
- Ostro, B., Goldberg, D., Hertz, A., Burnett, R.T., Shin, H., Hughes, E., Garcia, C., Henderson, K.D., Bernstein, L., Lipsitt, M. Assessing Long-Term Exposure in the California Teachers Study. *Environmental Health Perspectives* 2011;119: A242-A243. Erratum for: *Environ Health Perspect*. 118:363.
- Park, S., Ku, J., Lee, S.-M., Hwang, H., Lee, N., Kim, H., Yoon, K.-J., Kim, Y., Choi, S.Q., 2022. Potential toxicity of inorganic ions in particulate matter: Ion permeation in lung and disruption of cell metabolism. *Science of The Total Environment* 824, 153818.
- Pope, C.A., Thun, M.J., Namboodiri, M.M., Dockery, D.W., Evans, J.S., Speizer, F.E., Heath, C.W., 1995. Particulate air pollution as a predictor of mortality in a prospective study of US adults. *American journal of respiratory and critical care medicine* 151, 669–674.
- Popovicheva, O., Persiantseva, N., Kireeva, E., Khokhlova, T., Shonija, N., 2011. Quantification of the hygroscopic effect of soot aging in the atmosphere: laboratory simulations. *The Journal of Physical Chemistry A* 115, 298–306.
- Randles, C.A., da Silva, A.M., Buchard, V., Colarco, P.R., Darmenov, A., Govindaraju, R., Smirnov, A., Holben, B., Ferrare, R., Hair, J., Shinohara, Y., Flynn, C.J., 2017. The MERRA-2 Aerosol Reanalysis, 1980 Onward. Part I: System Description and Data Assimilation Evaluation. *J Climate* 30, 6823–6850.
- Rubasinghe, G., Lentz, R.W., Scherer, M.M., Grassian, V.H., 2010. Simulated atmospheric processing of iron oxyhydroxide minerals at low pH: roles of particle

- size and acid anion in iron dissolution. *Proceedings of the National Academy of Sciences* 107, 6628–6633.
- Schwartz, J.; Lepeule, J. Is ambient PM_{2.5} sulfate harmful? Schwartz and Lepeule Respond. *Environmental Health Perspectives* 2012;120:a454-a455.
- Thurston, G.D., Burnett, R.T., Turner, M.C., Shi, Y., Krewski, D., Lall, R., Ito, K., Jerrett, M., Gapstur, S.M., Diver, W.R., 2016. Ischemic heart disease mortality and long-term exposure to source-related components of US fine particle air pollution. *Environmental health perspectives* 124, 785–794.
- Wielicki, B.A., Barkstrom, B.R., Baum, B.A., Charlock, T.P., Green, R.N., Kratz, D.P., Lee, R.B., Minnis, P., Smith, G.L., Wong, T., 1998. Clouds and the Earth's Radiant Energy System (CERES): algorithm overview. *IEEE Transactions on Geoscience and Remote Sensing* 36, 1127–1141.
- Wu, S., Hao, J.-M., Lü, Z.-F., Zhao, Z., Li, J.-H., 2007. Effect of ammonium sulfate aerosol on the photochemical reaction of toluene/NO (x)/air mixture. *Huan Jing ke Xue=— Huanjing Kexue* 28, 1183–1187.
- Xing, J., Mathur, R., Pleim, J., Hogrefe, C., Gan, C.M., Wong, D.C., Wei, C., Gilliam, R., Pouliot, G., 2015. Observations and modeling of air quality trends over 1990–2010 across the Northern Hemisphere: China, the United States and Europe. *Atmospheric Chemistry and Physics* 15, 2723–2747.
- Xue, T.; Zhu, T.; Zheng, Y.X.; Liu, J.; Li, X.; Zhang, Q. Change in the number of PM_{2.5}-attributed deaths in China from 2000 to 2010: Comparison between estimations from census-based epidemiology and pre-established exposure-response functions. *Environment International* 2019;129:430-437.
- Yuan, X., Mi, M., Mu, R., Zuo, J., 2013. Strategic route map of sulphur dioxide reduction in China. *Energy Policy* 60, 844–851.
- Zhang, Q., Geng, G., 2019. Impact of clean air action on PM_{2.5} pollution in China. Springer.
- Zhao, Q., Zhao, W., Bi, J., Ma, Z., 2021. Climatology and calibration of MERRA-2 PM_{2.5} components over China. *Atmospheric Pollution Research* 12, 357–366.
- Zheng, B., Tong, D., Li, M., Liu, F., Hong, C.P., Geng, G.N., Li, H.Y., Li, X., Peng, L.Q., Qi, J., Yan, L., Zhang, Y.X., Zhao, H.Y., Zheng, Y.X., He, K.B., Zhang, Q., 2018. Trends in China's anthropogenic emissions since 2010 as the consequence of clean air actions. *Atmospheric Chemistry and Physics* 18, 14095–14111.